Polymer 73 (2015) 205–213

Contents lists available at ScienceDirect

Polymer

journal homepage: www.elsevier.com/locate/polymer

Thin film morphology and charge carrier mobility of diketopyrrolopyrrole based conjugated polymers

Deepak Chandran [a, *, 1, 2], Tomasz Marszalek [b, 1], Wojciech Zajaczkowski [b], Pramod Kandoth Madathil [a], Ratheesh K. Vijayaraghavan [c], Yun-Hyuk Koh [a], Sung-yeoun Park [a], Julian Robert Ochsmann [b], Wojciech Pisula [b, d], Kwang-Sup Lee [a, **]

[a] Department of Advanced Materials, Hannam University, Daejeon 305-811, South Korea
[b] Max Planck Institute for Polymer Research, 55128 Mainz, Germany
[c] Department of Chemical Sciences, Indian Institute of Science Education and Research Kolkata, Mohanpur 741246, India
[d] Department of Molecular Physics, Faculty of Chemistry, Lodz University of Technology, Zeromskiego 116, 90-924 Lodz, Poland

ARTICLE INFO

Article history:
Received 30 March 2015
Received in revised form
16 July 2015
Accepted 24 July 2015
Available online 26 July 2015

Keywords:
Diketopyrrolopyrole
Heteroatom substitution
Organic field effect transistors
Thin film morphology
Charge carrier mobility
Ambipolar polymer

ABSTRACT

A series of narrow bandgap donor–acceptor (D–A) type π-conjugated polymers consisting of thiophene (**Th**)- or furan (**Fu**)-flanked diketopyrrolopyrroles (**DPP**s) as acceptor units and thieno[3,2-*b*]thiophene (**TT**) or didodecyloxybenzo[1,2-*b*;3,4-*b*]dithiophene (**BDT**) moieties as donor units were synthesized. Cyclic voltammetry and UV–vis absorption studies revealed that both the heteroatom substitution in the aromatic end-groups of **DPP**s and variations in the chemical backbone influenced the bandgap of these polymers. The **TT**-based polymers showed a better thermal stability than their **BDT** analogs. **P(ThDPP-TT)** with better backbone planarity among the polymers being studied was found to organize in edge-on fashion on silicon/silicon dioxide surface, while all others showed a mixed type of both face- and edge-on arrangements. A substantial reduction in the thin film order and packing of the polymer chains was observed as the terminal thiophene units of **DPP** were replaced with furan. However, the furyl substituted polymer exhibited relatively high charge carrier mobility possibly due to improved conduction along the polymer backbone. The charge carrier transport properties of these polymers in organic field effect transistors (OFETs) were found to be influenced by incorporated donor units. Polymers with **BDT**-donor group exhibited unipolar hole transport, while those with **TT** units were ambipolar in nature. The present study demonstrates a systematic investigation of the structure–property relationships of D–A type **DPP** based π-conjugated copolymers which may enlighten better design strategy of polymers with novel chemical structures in the future.

© 2015 Elsevier Ltd. All rights reserved.

1. Introduction

Over the past few decades, organic field effect transistors (OFETs) have been extensively studied due to their enormous potential applications in large area displays, optical communication systems, sensors, radiofrequency identification tags, lighting and lasers [1–4]. Organic π-conjugated small molecules and polymers have been recognized as promising active layer materials for OFETs [1–8]. Previous reports have shown that solution processed donor–acceptor (D–A) copolymers satisfy OFET requirements better than vacuum deposited small molecules, which in general are characterized with poor patterning and structural defects derived device sensitivity [9,10]. The key feature of D–A copolymers is the enhancement of charge transport efficiency by tuning their frontier molecular orbital (FMO) energy levels [11]. Control over FMOs can result in n-type and p-type transistor operations using a single layer, an essential quality for complementary metal oxide semiconductor (CMOS) device applications [11–13]. Among various reported active materials for OFETs, dialkyl substituted diketopyrrolopyrrole (**DPP**) units have been identified as one of the most promising class of acceptor building blocks

* Corresponding author.
** Corresponding author.
E-mail addresses: deepak.chandran@dcu.ie (D. Chandran), kslee@hnu.kr (K.-S. Lee).
[1] Both authors have equal contribution.
[2] Present Address: School of Chemical Sciences & National Institute for Cellular Biotechnology, Dublin City University, Glasnevin, Dublin-9, Ireland.

http://dx.doi.org/10.1016/j.polymer.2015.07.043
0032-3861/© 2015 Elsevier Ltd. All rights reserved.

[14–21]. The ability of **DPP**s to extend spatial electronic overlap between adjacent monomers in a polymer chain facilitates rapid transport of charge carriers between the polymer chains [11,22]. Furthermore, **DPP** containing copolymers are known for high charge carrier mobilities and ambipolar properties owing to their ability to chemically tailor the ionization potential (IP), electron affinity (EA) and strong dipole moment in their unit structures [11,23–28], which makes them potential candidates for detailed structure–property relationship investigations [28–30].

Recent reports have examined atomistic bandgap engineering as a means to control FMO energy levels in conjugated donor–acceptor frameworks, especially the influence of thiophene to furan substitutions of organic π-conjugated materials [31–36]. However, substitution of thiophene with furan has garnered attention as a method to manipulate polymer planarity and crystallinity without much debate [31–36]. Park et al. has recently reported that the structure of the donor moiety is highly influential in determining the physical and electronic properties of D–A type conjugated polymers [37]. Given the number of modifications attempted in **DPP** based monomers to tune their molecular orbital (MO) energies and induce better crystallinity, a systematic investigation of the structure–property relationships with respect to their charge carrier mobility and molecular alignment in thin films remains limited [17,37–48]. Understanding the effect of specific structural changes of polymeric material on device properties is essential to facilitate the design and development of high performance polymers for future electronic applications.

In the present work, we have synthesized a series of narrow bandgap D–A type diketopyrrolopyrrole-*co*-thieno[3,2-*b*]thiophene or didodecyloxybenzo[1,2-*b*;3,4-*b*]dithiophene copolymers: **P(ThDPP-TT)**, **P(ThDPP-BDT)**, **P(FuDPP-TT)**, and **P(FuDPP-BDT)** (Fig. 1) through Pd-catalyzed Stille coupling reactions. Using these polymers, we have investigated the influence of (i) variation in the chemical structure by heteroatom substitution of terminating aromatic heterocyclics of **DPP** and (ii) the π-extension of thiophene based donor monomer units on various properties such as the solubility, thermal properties, FMO energy levels, polymer chain alignment on surfaces and the charge carrier transport properties in OFETs. One of the key outcomes from our studies is a demonstration that the structure of the donor monomeric units in **DPP**-based polymers has substantial influence in determining the type of device operation (ambipolar or unipolar) and the efficacy of charge transport in thin films. Additionally, we found that the decrease in the peripheral steric demand on the polymer backbones causing a preferential face-on organization to shift towards an edge-on organization in thin films. This study does not focus on achieving neither novel copolymer structures nor record mobilities but instead demonstrates a systematic investigation of the structure–property relationships of D–A type π-conjugated **DPP**-based polymers which may pave the way towards improved design strategies of polymers with novel chemical structures in the future.

2. Results and discussion

2.1. Synthesis

Heteroaromatic substitutions in **DPP** acceptor monomers are tailored in such a way that the terminating thiophene (with large sulfur atom) is replaced by furan (with small oxygen atom). We made this structural alteration with an expectation that in a similar crystal lattice state, the smaller atomic radius of oxygen can lead to a decrease in intermolecular distances and hence it would result in better packing of the copolymer chains [49]. In the case of donor monomers, thieno[3,2-*b*]thiophene and its one-dimensional π-extended structure didodecyloxybenzo[1,2-*b*;3,4-*b*]dithiophene were attempted with an expectation that efficient π–π stacking could be possible in the case of latter monomer unit [50]. All these copolymers were end capped to avoid charge trapping and hence to increase the device performances as known in literature [51–53].

The chemical structures of the investigated copolymers are compiled in Fig. 1. All the polymers were synthesized by Stille cross-couplings reactions and isolated as dark green solids having high molecular weights with excellent mass recovery (see M_n and PDI values below). Detailed synthetic procedures and characterization data can be found in the Experimental section (Supporting information). Polymer **P(ThDPP-TT)** hosting long pendant alkyl chains was prepared by cross coupling reaction of thienyl-**DPP** (**ThDPP**) and thieno[3,2-*b*]thiophene (**TT**) monomers. **P(FuDPP-TT)** represents the furyl-**DPP** (**FuDPP**) analog of **P(ThDPP-TT)**. Similarly, **P(ThDPP-BDT)** and **P(FuDPP-BDT)** represent the combination of thienyl- and furyl-**DPP**s with didodecyloxybenzo[1,2-*b*;3,4-*b*]dithiophene (**BDT**) based donor monomers. The furyl-**DPP**

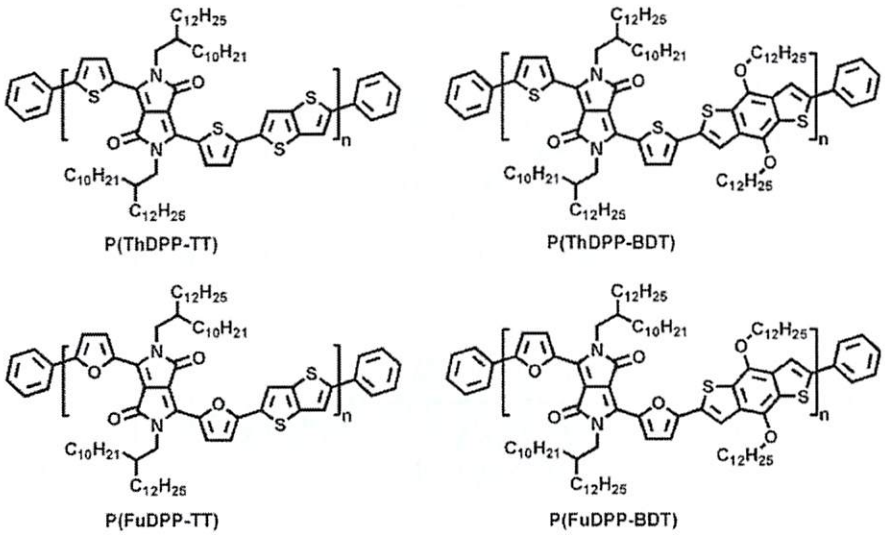

Fig. 1. Chemical structures of **DPP** based polymers.

polymers exhibited higher solubility compared to their thienyl analogs. It has been reported that the ratio of furan to thiophene could determine the solubility of polymers with mixed heterocycle backbones and dramatically reduce the amount of aliphatic side-chain material necessary to solubilize polymers [54,55]. In our furan substituted polymers, in addition to a higher furan to thiophene ratio, presence of long as well as large amount of alkyl chain remarkably improved the solubility. **P(ThDPP-TT)**, **P(ThDPP-BDT)** and **P(FuDPP-TT)** were soluble in chlorinated solvents such as dichloromethane, chloroform and chlorobenzene, whereas polymer **P(FuDPP-BDT)**, with a combination of higher alkyl and alkoxy chain density and higher thiophene-furan ratio exhibited solubility even in *n*-hexane.

GPC analysis in tetrahydrofuran (THF) at 40 °C lead to overestimation of molecular weights (M_n for **P(ThDPP-TT)** ¼ 33 kDa) compared to that in 1,2,4-*trichlorobenzene* (TCB) at 135 °C (M_n for **P(ThDPP-TT)** ¼ 29 kDa). This is attributed to the rigid conformation of the polymer chains adopted in THF solution [56]. In addition to that, **DPP**-based copolymers of fused thiophenes tend to aggregate in solution and the dissolution of these aggregates occurs only at high temperatures (>200 °C) [57]. The relatively higher polydispersities of our polymers could be due to the fairly lower temperature used for the GPC analysis. The M_n of polymers **P(ThDPP-TT)**, **P(FuDPP-TT)**, **P(ThDPP-BDT)** and **P(FuDPP-BDT)** measured in TCB were 29 kDa (PDI ¼ 4.90), 22 kDa (PDI ¼ 4.60), 26 kDa (PDI ¼ 5.39) and 13 kDa (PDI ¼ 3.87) respectively.

2.2. Optical and electrochemical properties

The optical characteristics of the polymers were investigated by UV–vis absorption spectroscopy. The spectra were recorded for both chlorobenzene solution and for spin coated film on quartz plates. Fig. 2a and b show the individual absorption spectral profiles of all polymers in chlorobenzene solution and films, respectively. All the polymers exhibited almost similar absorption profiles with two primary absorption bands in both solution and film. These bands are typical for **DPP** based polymers with less intense high energy and more intense low energy transitions attributed to $\pi-\pi^*$ and intramolecular charge transfer (ICT) transitions respectively. λ_{max} for the $\pi-\pi^*$ transition for **P(ThDPP-TT)** polymer was observed at ~424 nm, while for **P(ThDPP-BDT)**, **P(FuDPP-TT)** and **P(FuDPP-BDT)** at around 420 nm, 412 nm and 398 nm, respectively. λ_{max} for lower energy ICT bands were observed at ~797 nm, 735 nm, 791 nm and 743 nm, respectively, for **P(ThDPP-TT)**, **P(ThDPP-BDT)**, **P(FuDPP-TT)** and **P(FuDPP-BDT)**. In general, polymers with **TT** monomers exhibited a very similar absorption spectral profile, while those with **BDT** monomers exhibited a blue shifted profile. This blue shift in absorption spectral maxima could be attributed to their non-planar backbones (for **BDT**s) relative to the **TT** based polymers. In the case of thienyl-**DPP** polymers, the CT absorption bands in the film state were observed to be broadened and red-shifted relative to the absorption maxima in their solution state. In contrast, a slight blue-shift in the absorption spectral maxima was observed for the furyl-**DPP** polymers due to the depleted aromaticity of furans relative to that of thiophenes [58,59]. Small vibrational splitting shoulders appear for all polymers (Fig. 2b). The optical bandgaps (E_g) of all polymers were determined from their optical absorption onsets (λ_{onset}). **P(ThDPP-BDT)** has the lowest E_g (1.28 eV), while **P(FuDPP-BDT)** showed the highest E_g (1.43 eV) values in chlorobenzene solution. The other two polymers, **P(ThDPP-TT)** and **P(FuDPP-TT)**, exhibited intermediate E_g of 1.33 and 1.39 eV, respectively. The E_g values of similar polymers with shorter 2-octyldodecyl or analogous 2-decyltetradecyl side chains on **DPP**s have been reported in the range 1.3–1.9 eV [18,46,48,60–64]. A few recently reported **DPP** based molecular materials showed insignificant influence of

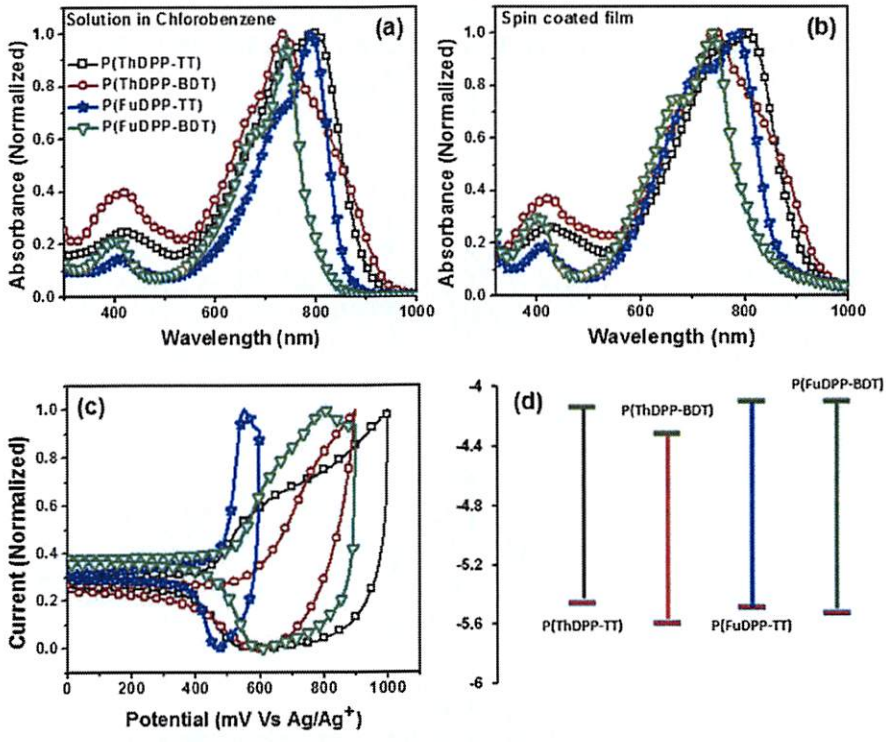

Fig. 2. UV–Vis absorption spectra recorded in a) solution of chlorobenzene and b) thin film, c) cyclic voltammogram (CV) of the polymers; potentials relative to Ag/Ag^b (calibrated against Fc/Fc^b) d) HOMO and LUMO energy levels of the polymers determined from UV–Vis and CV.

heteroatom substitution on their optical absorption profiles [33–35]. Nguyen and coworkers have reported that heteroatom substitutions in the aromatic remote end-groups (thiophene to furan) in **DPP**-based molecular materials has been observed to manipulate solubility, thermal properties, film morphology and charge carrier mobility significantly, but the optical absorption and frontier orbital energy levels were remained less influenced [33]. A similar observation is also reported in a closely resembling Pechmann dye system where these substitutions at the remote ends resulted in similar E_g values [35]. In our studies, we have made a similar heteroatom substitution in the closely flanking aromatic rings of **DPP**s instead of their remote ends. Interestingly, we have observed 0.15 eV and 0.06 eV increase in the bandgap of **BDT** and **TT** based polymers, respectively.

The FMO energies were derived from absorption onsets of the UV–vis spectra and the cyclic voltammograms. Fig. 2c shows the cyclic voltammograms of all the four polymers during oxidative scan. The oxidation onset potential ($E_{ox,onset}$) of **P(ThDPP-TT)**, **P(FuDPP-TT)**, **P(ThDPP-BDT)** and **P(FuDPP-BDT)** were 0.44, 0.49, 0.59 and 0.52 V, respectively, when measured relative to Ag/Ag^{+} (calibrated against to Fc/Fc^{+} redox couple). The HOMO energy values were calculated using $E_{ox,onset}$ according to the previously reported procedures [65]. The LUMO energy levels of the polymers were estimated from the film state E_g and the HOMO energy level. The calculated HOMO and LUMO energy levels of the polymers are summarized in Fig. 2d and in Table 1, indicating that the influence of heteroatom substitution is less prominent, while the impact of the donor monomers is significant on the FMO of the polymers. The observed LUMO levels are deeper than the previously reported values for the shorter (on **DPP**) or branched side chain (on **BDT**) analogs of these polymers [61,66]. When the donor unit is changed from **TT** to **BDT**, a small reduction in the HOMO and LUMO energy values (by 0.13 eV and 0.18 eV respectively) were observed for both **P(ThDPP-TT)** and **P(ThDPP-BDT)**. A less proficient reduction in the HOMO level (by 0.04 eV) occurred between **P(FuDPP-TT)** and **P(FuDPP-BDT)**, however, the LUMO energy remained unchanged. The thiophene to furan substitution in **TT** based polymers (**P(ThDPP-TT)** and **P(FuDPP-TT)**) engendered an insignificant changes in HOMO (0.02 eV decrease) and LUMO (0.04 eV increase) values. A similar substitution in **BDT** based polymers (**P(ThDPP-BDT)** and **P(FuDPP-BDT)**) revealed an increase in HOMO (0.07 eV) and LUMO (0.22 eV) values. Thiophene-furan substitutions were expected with a significant lowering of HOMO energy levels due to the decrease in electron density attributed to the higher ionization potential of furan [31]. But in our case we have not seen any considerable influence of these substitutions on HOMO values. This is probably due to the HOMO and LUMO orbitals that received higher contribution from the central **DPP** core and the influence of closely flanking heteroaromatics are less in the FMOs [35].

2.3. Thermal properties

Thermogravimetric analysis (TGA) was performed at a heating rate of 10 °C/min under N_2 atmosphere in order to gain insight in to the thermal and/or oxidative stabilities of the polymers. The results for thieno[3,2-*b*]thiophene donor monomer based polymers, **P(ThDPP-TT)** and **P(FuDPP-TT)**, indicated that the polymers started to thermally degrade at around 370 °C. The **BDT** based polymers **P(ThDPP-BDT)** and **P(FuDPP-BDT)** exhibited a relatively lower thermal stability with an onset of thermal degradation temperature at around 290 °C. The maximum decomposition rate for all these polymers were occurred at around 450 °C regardless of the structure of the donor monomer. Differential scanning calorimetry (DSC) was used to determine phase transition characteristics of the **ThDPP** based polymers. The endothermic transition temperature at 260 °C during the first heating scan of **P(ThDPP-TT)**, could be attributed to the melting of the polymer backbone. The absence of melting of the side chains indicates that the crystallization of the polymer main chain dominates whereas crystallization of the long, branched 2-decyltetradecyl side chains is forbidden, during the polymer packing [67]. There were no corresponding exothermic peaks in the subsequent cooling scan and the endothermic peaks disappeared during the second heating scan. Polymer **P(ThDPP-TT)** showed quite similar DSC profiles with endothermic transition at 260 °C in the first heating scan and no corresponding exothermic peaks in the subsequent cooling scan.

2.4. Investigation of polymer organization

To understand the influence of the chemical structure of the donor and acceptor units on the self-organizing nature of the polymers on surfaces, grazing incidence wide-angle X-ray scattering (GIWAXS) measurements were performed. All samples were spin-coated from o-dichlorobenzene solution with a polymer concentration of 10 mg/mL. To remove residual solvent and improve the order in films, thermal annealing at 300 °C was applied (see more information about sample preparation in the Supporting information). The polymer arrangement on the dielectric surface as well as interlayer and π-stacking distances was summarized in Table 2.

The GIWAXS patterns indicated a significant difference between the **P(ThDPP)** polymers with various donor-**TT** and **-BDT** groups

Table 1
Optical and electrochemical properties of polymers.

Polymer	Optical properties[a]								Electrochemical properties[e] & FMOs		
	Solution[b]				Film[c]						
	π/π^*	ICT		E_g[d] (eV)	π/π^*	ICT		E_g[d] (eV)	E_{ox}[e] (V)	HOMO[f] (eV)	LUMO[g] (eV)
	λ_{max} (nm)	λ_{max} (nm)	λ_{onset} (nm)		λ_{max} (nm)	λ_{max} (nm)	λ_{onset} (nm)				
P(ThDPP-TT)	424	797	918	1.35	434	808	935	1.33	0.44	−5.47	−4.14
P(ThDPP-BDT)	420	735	942	1.32	430	750	972	1.28	0.59	−5.60	−4.32
P(FuDPP-TT)	412	791	875	1.41	415	785	890	1.39	0.49	−5.49	−4.10
P(FuDPP-BDT)	398	743	842	1.47	401	737	869	1.43	0.52	−5.53	−4.10

[a] From UV–vis spectra.
[b] In chlorobenzene at rt.
[c] Spin cast on quartz plate.
[d] E_g ¼ 1240/λ_{onset}.
[e] From CV.
[f] E_{HOMO} ¼ −(Eonset, ox vs Fc=Fc+ þ 5:1)eV; [65].
[g] E_{LUMO} ¼ E_{HOMO} þ E_g.

Table 2
Summary of the interlayer and π-stacking distances of the polymers as determined by GIWAXS.* The term hybrid' indicated a mixed arrangement of the polymer chains with face-on and edge-on surface organization.

Polymer	Interlayer distance (nm)	π-stacking distance (nm)	Surface organization
P(ThDPP-TT)	2.14	0.37	Edge-on
P(ThDPP-BDT)	2.35	0.38	Hybrid*
P(FuDPP-TT)	2.11	0.41	Hybrid*
P(FuDPP-BDT)	2.22	0.39	Hybrid*

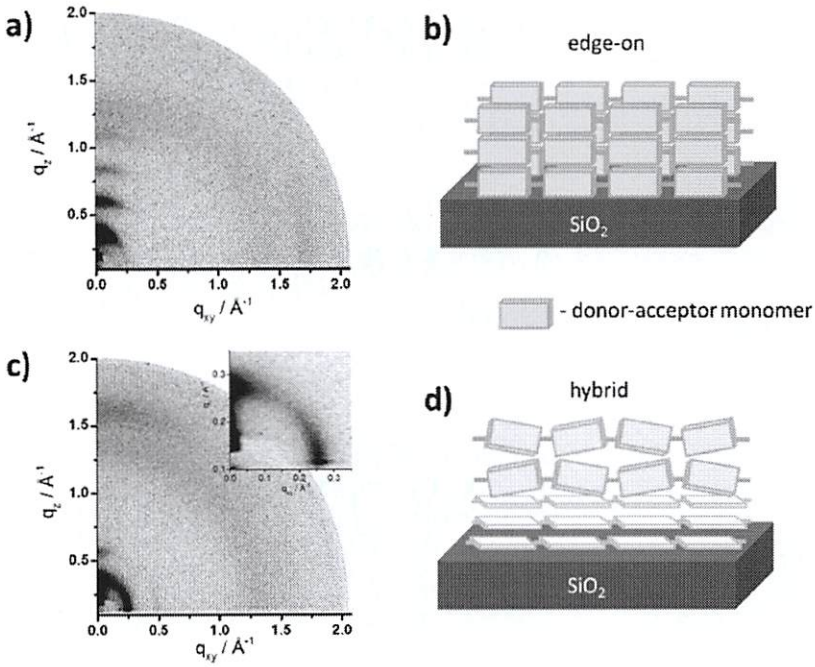

Fig. 3. GIWAXS patterns of films based on a) **P(ThDPP-TT)** and c) **P(ThDPP-BDT)** (inset corresponds to the small-angle region). Schematic illustrations of the polymer packing with b) edge-on of **P(ThDPP-TT)** and d) hybrid arrangement of **P(ThDPP-BDT)**.

(Fig. 3a and c) in surface arrangement. The **P(ThDPP-TT)** film exhibited a high degree of order in the meridional plane (along q_z for q_{xy} ¼ 0 Å^{-1}) as indicated by reflections up to fourth order (Fig. 3a). The interlayer distance of 2.14 nm was determined from the main peak position on the meridional plane. This value was in agreement with the theoretical polymer width including alkyl chains as determined by Cerius^2 calculations (Fig. S15). The wide-angle equatorial scattering intensity was assigned to a π-stacking distance of 0.37 nm of edge-on arranged conjugated backbones (Fig. 3a) [68]. These values are very similar to the spacings recently found for octyldodecyl substituted **P(ThDPP-TT)** [60]. The GIWAXS pattern of **P(ThDPP-BDT)** suggested a lower packing order of the polymer chain than in the case as described before (Fig. 3b). This was evident from the weak peak intensity, lack of higher order reflections, larger full-width-at-half-maximum values of the scattering intensities and the isotropic-like angular intensity distribution of the first small-angle feature corresponding to the interlayer spacing of 2.35 nm. Interestingly, this reflection has a maximum intensity located on both the equatorial and meridian plane as apparent from the low contrast pattern of the small-angle region (inset in Fig. 3c) indicated a mixed face-on and edge-on organization. Additionally, the π-stacking peak attributed to a distance of 0.38 nm emerged on the meridional plane at q_{xy} ¼ 0 Å^{-1} and q_z ¼ 1.65 Å^{-1} suggested a preferential face-on arrangement of the polymer on the surface. The low order observed for the **BDT**-based polymer is in agreement with similar systems based on dithieno**BTZ-DPP** [69].

Replacing the thiophene units with furan has been reported to impact the polymer chain order and inter-lamellar packing in films [49], but in the same time to increase solubility [55]. In this work, both the furan-based **P(FuDPP)** polymers with **TT** and **BDT** donor groups, resulted in poor packing order as evaluated from their thin film GIWAXS results (Fig. 4a, b). Identical packing behavior was reported for dioctadecyl-substituted **P(FuDPP-TT)** [64] or for furan-**DPP** polymers containing naphthalene or anthracene [70] instead of **TT** in the backbone. On the other hand, replacing **TT** by an additional furan unit results in good packing in thin films [71]. The π-stacking increased to 0.41 nm for **P(FuDPP-TT)** and 0.39 nm for **P(FuDPP-BDT)** in comparison to their thiophene analogs. As discussed above for **P(ThDPP-BDT)**, both furan-based **P(FuDPP)** polymers were found to arrange in a hybrid fashion with mixed domains of face-on and edge-on alignment. Similar to **P(ThDPP-BDT)**, the face-on oriented furan-based **P(FuDPP)** polymers were found to be packed in layer structures which were not well organized towards each other (Fig. 4a, b). This was obvious from the lack of equatorial small-angle reflections which were expected to be present together with the meridional peak corresponding to π-stacking. On the other hand, the edge-on aligned layers exhibited improved order as confirmed from meridional scattering intensities up to 3rd order. However, the lack of equatorial wide-angle

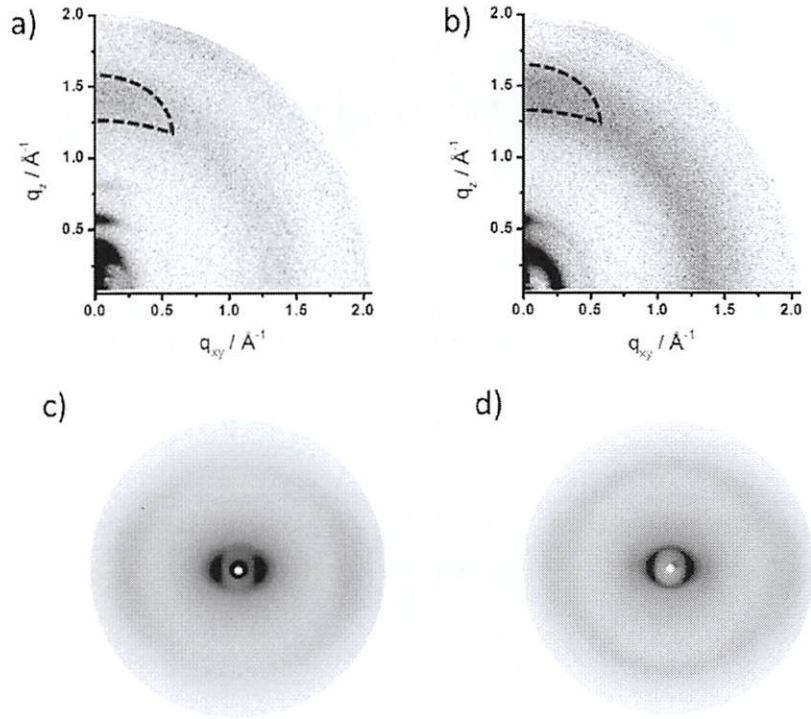

Fig. 4. GIWAXS patterns of thin films of a) **P(FuDPP-TT)** and b) **P(FuDPP-BDT)**, reflections related to π-stacking are indicated by dashed circles. 2DWAXS patterns of c) **P(FuDPP-TT)** and d) **P(FuDPP-BDT)** recorded at 30 °C.

reflections corresponding to the π-stacking clearly indicated a disordered packing of the polymer chains. To further verify the polymer organization and to exclude artifacts in the GIWAXS patterns, two dimensional wide angle X-Ray scattering (2DWAXS) measurements on extruded, macroscopically aligned fibers were performed for both **P(FuDPP-TT)** and **P(FuDPP-BDT)**. The 2DWAXS patterns indicated a characteristic distribution of the two scattering features of uniaxially oriented polymer chains, the reflection corresponding to (i) π-stacking and (ii) interlayer distances, both were positioned only on the equatorial plane (Fig. 4c, d). This confirmed that the meridional peaks in the GIWAXS patterns were indeed related to the π-stacking of the polymers. The spacings in the bulk are in agreement with the values found in the thin films. This suggests that the polymer–substrate interaction did not significantly change the organization in thin film.

The analysis of the data revealed significant differences between **P(ThDPP-TT)** and the three other polymers. In comparison to the clear edge-on organization of **P(ThDPP-TT)** on the surface, **P(ThDPP-BDT)** was arranged in a more complex fashion and in the same way as **P(FuDPP-TT)** and **P(FuDPP-BDT)**. In one part of the domains, the backbones were face-on oriented as verified by the locations of the π-stacking reflection on the meridional and the interlayer correlation on the equatorial plane of the GIWAXS pattern. However, the additional appearance of meridional interlayer features indicated that in some domains the polymer backbones were organized also in an edge-on fashion. Since an equatorial scattering intensity for the π-stacking was missing, the **P(ThDPP-BDT)** polymer chains were weakly packed in these edge-on domains. The furan-based polymers **P(FuDPP-TT)** and **P(FuDPP-BDT)** showed an identical mixed organization. In the film, the domains of different organization might be e.g. phase separated horizontally with the face-on arranged polymer close at the interface to the dielectric, while the bulk film could consist of edge-on aligned, but poorly packed **P(ThDPP-BDT)**. Such hybrid orientations in polymer films have been observed for several high performing polymers such as naphthalene–dicarboximide–bithiophene [72] and siloxane-terminated isoindigo-based conjugated polymers [73]. However, a close relation between polymer design, packing and surface arrangement as in our work was still missing. This understanding is important since the surface arrangement has great influence on the charge carrier transport in transistors. For instance, in an edge-on organization the π-stacking direction was parallel to the substrate, typically favoring the migration of charge carriers, while in the face-on case the stacking was oriented perpendicular to the surface with in-plane aligned alkyl side chains hindering the transport. The variation in surface organization between **P(ThDPP-TT)** and **P(ThDPP-BDT)** was related to the difference in the donor units **TT** and alkyl substituted **BDT**, which affected the backbone planarity and polymer packing. The literature evaluation exposed a certain trend that macromolecules with a low backbone planarity arranged face-on, while well-packed planar systems oriented edge-on towards the surface. One prominent example is **P3HT** which exhibited a face-on organization for the low regioregular, non-planar polythiophene derivate and edge-on in the high regioregular case [74]. Another very recent report described a similar self-assembling behavior for benzotrithiophene-based polymers with and without sterically demanding alkyl substituents [75,76]. In our work, we closely correlated the degree of packing for polymers of varied backbone twisting with the type of surface organization and revealed the coexistence of domains of mixed arrangement. The introduction of the **BDT** unit in the backbone increased the peripheral steric demand and decreased the planarity of the system. This was further confirmed by the above absorption spectra of the films as **BDT** based polymers exhibited a blue shifted λ_{max} (750 and 737 nm) relative to that of **TT** polymers (808 and 785 nm). This was in

agreement with the lower order and slightly larger π-stacking distance in the solid-state of these polymers. In domains with the face-on arrangement, the π-stacking direction was perpendicular to the applied field (normal to the surface) which might hinder the charge carrier transport and thereby lower the device performance as discussed in the next section. The **TT** unit rather leads to higher planarity, better packing accompanied with higher order and thus to an edge-on arrangement on surfaces. A better planarity of the polymer chains resulted in stronger interchain interaction and ultimately decreased the solubility of the compound. It has been recently shown for poly(bifuran-furan-diketopyrrolopyrrole) that a reduced backbone planarity leads to low aggregation in solution which seems to be the main driving force for the face-on orientation [71]. In contrast to this, formation of large aggregates of strongly interacting polymers favors an edge-on organization.

2.5. Charge carrier transport in transistors

All polymers were cast under the same experimental conditions used for the structural characterization by GIWAXS (Si/SiO_2 substrate without surface modification) as the active layers for bottom contact, bottom gate OFETs. All four polymers **P(ThDPP-TT)**, **P(ThDPP-BDT)**, **P(FuDPP-TT)** and **P(FuDPP-BDT)** exhibited clear field-effect characteristics under the used device configuration (Table 3). Three factors were identified bearing an impact on the device operation: 1) chemical design of donor and acceptor, 2) π-stacking distance and intrachain transport, 3) polymer surface organization and order. As reported in literature, the charge carrier mobility of **P(ThDPP-TT)**-based polymers in transistors is influenced by molecular weight and length of the alkyl substituents with value variations between around $10^{\square 2}$ cm^2/V s for hexyldecyl [61] and 1.0 cm^2/V s for octyldodecyl [18] side chains.

In terms of point 1) it was found that polymers containing **BDT** as a donor group demonstrated a unipolar hole transporting behavior, while compounds with the **TT** donor unit showed ambipolarity. Though the ambipolarity of the **TT** polymers were not fully apparent from the transistor output curves (which were in linear scale), the ambipolar device characteristics were evident from the transfer plots (in log scale). The reason for such behavior was a difference in injection rates between electrons and holes from metal electrodes to active layer. It is known that the type of device operation of octyldodecyl substituted **P(ThDPP-TT)** strongly depends on the work function of the electrodes. Optimization of the work function towards the polymer energy allows balanced electron and hole transport with mobilities above 1 cm^2/V s [18]. Since both **BDT**-based polymers did not exhibit an electron transport similar to the dithieno **BTZ-DPP** system [69], the ambipolar nature was exclusively associated to the chemical structure of the incorporated donor unit. As a next step, the influence of the chemical structure of the acceptor group on the device performance was investigated on the basis of the polymer pair **P(ThDPP-TT)** and **P(FuDPP-TT)**. Fig. 5a, b summarizes the output and transfer characteristics for **P(ThDPP-TT)** and Fig. 6 that of **P(FuDPP-TT)**. Relatively high contact resistance was obvious for **P(FuDPP-TT)** on the output and transfer characteristics and were related to structural disorder at the electrodes. The hole mobility of both polymers were in an identical range in bottom contact, bottom gate device configuration with μ_h ¼ 9 □ $10^{\square 2}$ cm^2/V s for **P(ThDPP-TT)** and μ_h ¼ 4 □ $10^{\square 2}$ cm^2/V s for **P(FuDPP-TT)**. These observations suggested that the hole transport was less dependent on the acceptor unit of the polymer, rather on the chemical structure of the donor unit.

To clarify the role of the π-stacking distance and intrachain transport from point 2) for this polymer series, the two polymers **P(ThDPP-TT)** and **P(FuDPP-TT)** were discussed in greater detail. The charge carrier mobility did not correlate with the π-stacking of

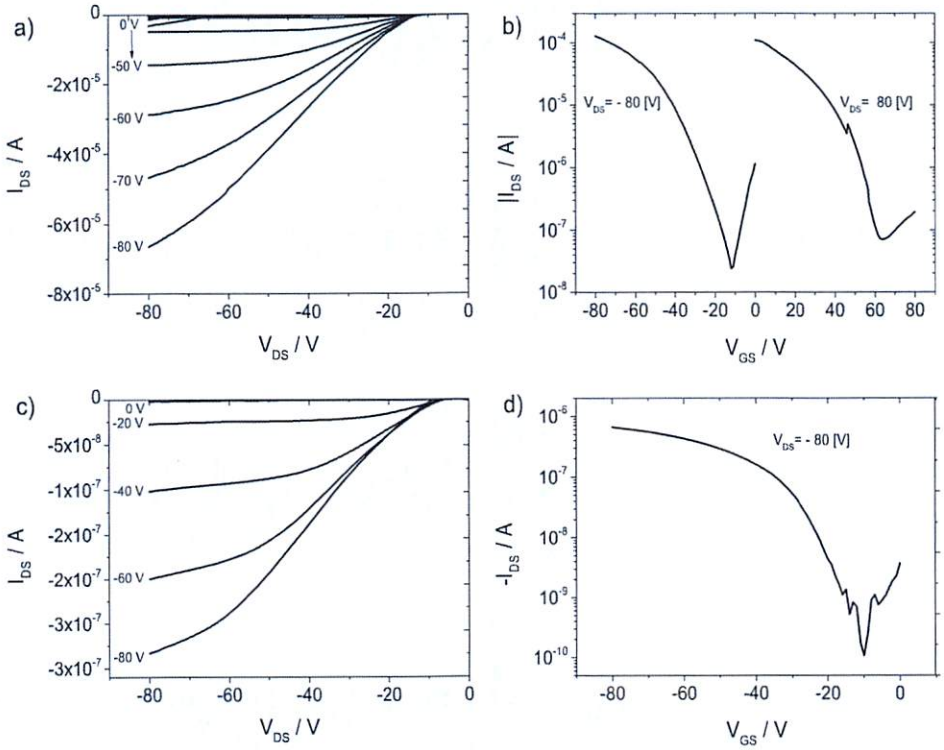

Fig. 5. Output and transfer characteristics of a) and b) **P(ThDPP-TT)** and c) and d) of **P(ThDPP-BDT)**.

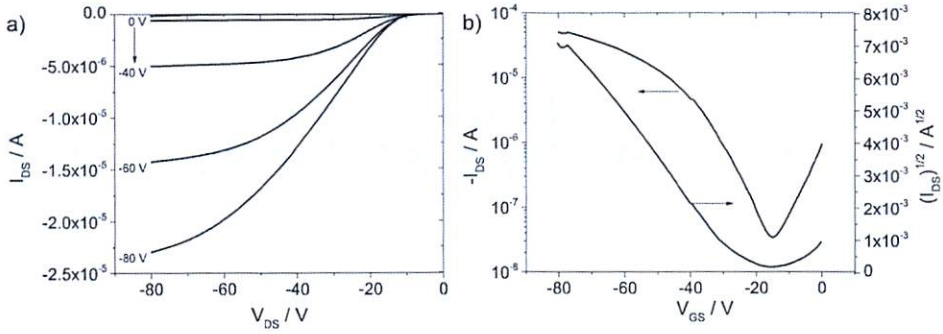

Fig. 6. OFET a) output and b) transfer characteristic of **P(FuDPP-TT)**.

Table 3
Parameters for bottom contact, bottom gate configuration transistors on not-modified SiO_2 surface.

Polymer	p-type		n-type	
	Mobility [cm^2/V s]	Threshold voltage [V]	Mobility [cm^2/V s]	Threshold voltage [V]
P(ThDPP-TT)	9 □ 10□2	□26	2 □ 10□4	þ45
P(ThDPP-BDT)	6 □ 10□4	□16	–	–
P(FuDPP-TT)	4 □ 10□2	□24	7 □ 10□4	þ50
P(FuDPP-BDT)	1 □ 10□3	□13	–	–

the polymers in the expected fashion since packing distances of 0.37 nm for **P(ThDPP-TT)** and 0.41 nm for **P(FuDPP-TT)** were determined. Thereby, the latter polymer revealed only half order of magnitude lower mobility suggesting a higher intrinsic charge carrier mobility. The fast, band-like conduction of charge carriers took place through the conjugated backbone, while the chain to chain hopping occurred by intermolecular overlapping of the π-orbitals of neighboring polymer chains. Since a larger π-stacking distance seriously reduced the hopping between **P(FuDPP-TT)** chains, the band-like conduction along the backbone needed to be significantly larger than for **P(ThDPP-TT)** in order to yield identical mobility values. This behavior could be explained by application of furan as a part of the donor units improving the hole transport in OFETs [77]. This trend was more evident for polymers with the **BDT** acceptor group, even when the molecular weight of **P(ThDPP-BDT)** was almost three times higher than **P(FuDPP-BDT)** with μ_h ¼ 6 □ $10^{□4}$ cm^2/V ς for **P(ThDPP-BDT)** and μ_h ¼ 1 □ $10^{□3}$ cm^2/V s for **P(FuDPP-BDT)**.

As the final factor the impact of polymer organization and order in thin films (point 3) on the charge carrier mobility was investigated on the example of **P(ThDPP-TT)** and **P(ThDPP-BDT)**. Hole mobilities of μ_h ¼ 9 □ $10^{□2}$ cm^2/V s for **P(ThDPP-TT)** and μ_h ¼ 6 □ $10^{□4}$ cm^2/V s for **P(ThDPP-BDT)** were extracted. In comparison to the edge-on arranged **P(ThDPP-TT)**, the hole carrier transport for the face-on oriented polymer bearing the **BDT** unit was found to be two orders of magnitude lower. The dramatic decrease in performance was related directly to the lower order, slightly larger π-stacking distance and perpendicular orientation of the stacking of the polymer chain backbone towards the charge carrier migration. In the face-on orientation, the alkyl side chains were oriented in-plane additionally hindering the transport.

3. Conclusions

In summary, we designed and synthesized a series of D–A type copolymers of **DPP**s with systematically varying backbone structure. The effect of both the donor unit variation and thiophene to furan substitution in **DPP** acceptor units on the bandgap, FMO, thin film organization and charge carrier transport were studied comprehensively. Although the influence of heteroatom substitution clearly altered the FMOs of **BDT**-polymers, its effect on **TT**-polymers was less pronounced. Moreover, a clear trend in the self-organization of the polymers on surfaces cannot be drawn based on the systematic variation of the structures as inferred from GIWAXS measurements. An attempt to increase the performance of the polymers by increasing π-extension in donor monomers from **TT** to **BDT** resulted into an increase of peripheral steric demand on polymer backbone. This is attributed to the presence of alkoxy-groups in **BDT** which lead to low aggregation in solution and finally to a face-on orientation in their thin films. As a result, the hole carrier transport in the face-on oriented **BDT** based co-polymers was found to be two orders of magnitude lower than that in the edge-on arranged **TT** copolymers. Another striking observation is that the ambipolar nature is exclusively associated to the chemical structure of the incorporated donor unit. This investigation ensures that the furans in polymer backbone give the advantage of band-like conduction of charge carriers which significantly determines the mobility values in their thin film devices. The present study provides a broad insight towards structure–property relationship on heteroatom substitution and selection of donor monomer in D–A type polymers which defines the polymer organization and order in thin films as well as the nature (ambipolar or unipolar) and the efficiency of the charge transport.

Acknowledgments

This study was partly supported by the Active Polymer Center for Pattern Integration (ERC R11-2007-050-01001) through the National Research Foundation of Korea. Authors acknowledge Prof. Klaus Müllen for his critical comments. T.M. and W.Z acknowledge the ERC Advanced Grant NANOGRAPH (AdG-2010-267160). D.C. acknowledges postdoctoral fellowship of the BK21 program from the Ministry of Education and Human Resources Development, Korea. DC also acknowledges the assistance provided by Dr. Jaemin Lee with CV measurements, Dr. R. P. Johnson for GPC measurements in THF, Dr. Rajani K. V for suggestions and criticism and Tadhg McGivern for reading the manuscript.

Appendix A. Supporting information

Supporting information related to this article can be found at http://dx.doi.org/10.1016/j.polymer.2015.07.043.

References

[1] Z. Bao, J. Locklin, Organic Field-effect Transistors, Taylor & Francis, 2007.
[2] H. Klauk, Chem. Soc. Rev. 39 (2010) 2643–2666.
[3] P. Lin, F. Yan, Adv. Mater. 24 (2012) 34–51.
[4] Y. Li, P. Sonar, L. Murphy, W. Hong, Energy Environ. Sci. 6 (2013) 1684–1710.
[5] A. Facchetti, M.H. Yoon, T.J. Marks, Adv. Mater. 17 (2005) 1705–1725.
[6] C.D. Dimitrakopoulos, P.R.L. Malenfant, Adv. Mater. 14 (2002) 99–117.
[7] S. Allard, M. Forster, B. Souharce, H. Thiem, U. Scherf, Angew. Chem. Int. Ed. 47 (2008) 4070–4098.
[8] J. Terao, A. Wadahama, A. Matono, T. Tada, S. Watanabe, S. Seki, T. Fujihara, Y. Tsuji, Nat. Commun. 4 (2013) 1691.
[9] Y. Deng, Y. Chen, X. Zhang, H. Tian, C. Bao, D. Yan, Y. Geng, F. Wang, Macromolecules 45 (2012) 8621–8627.
[10] M. Zhang, H.N. Tsao, W. Pisula, C. Yang, A.K. Mishra, K. Müllen, J. Am. Chem. Soc. 129 (2007) 3472–3473.
[11] C.R. Newman, C.D. Frisbie, D.A. da Silva Filho, J.-L. Brédas, P.C. Ewbank, K.R. Mann, Chem. Mater. 16 (2004) 4436–4451.
[12] R.J. Baker, CMOS: Circuit Design, Layout, and Simulation, Wiley, 2011.
[13] E.J. Meijer, D.M. de Leeuw, S. Setayesh, E. van Veenendaal, B.H. Huisman, P.W.M. Blom, J.C. Hummelen, U. Scherf, J. Kadam, T.M. Klapwijk, Nat. Mater. 2 (2003) 678–682.
[14] H. Chen, Y. Guo, G. Yu, Y. Zhao, J. Zhang, D. Gao, H. Liu, Y. Liu, Adv. Mater. 24 (2012) 4618–4622.
[15] J.S. Lee, S.K. Son, S. Song, H. Kim, D.R. Lee, K. Kim, M.J. Ko, D.H. Choi, B. Kim, J.H. Cho, Chem. Mater. 24 (2012) 1316–1323.
[16] M. Kaur, S.D. Yang, J. Shin, W.T. Lee, K. Choi, J.M. Cho, H.D. Choi, Chem. Commun. 49 (2013) 5495–5497.
[17] H. Bronstein, Z. Chen, R.S. Ashraf, W. Zhang, J. Du, J.R. Durrant, P. Shakya Tuladhar, K. Song, S.E. Watkins, Y. Geerts, M.M. Wienk, R.A.J. Janssen, T. Anthopoulos, H. Sirringhaus, M. Heeney, I. McCulloch, J. Am. Chem. Soc. 133 (2011) 3272–3275.
[18] Z. Chen, M.J. Lee, R.S. Ashraf, Y. Gu, S.A. Seifried, M.M. Nielsen, B. Schroeder, T.D. Anthopoulos, M. Heeney, I. McCulloch, H. Sirringhaus, Adv. Mater. 24 (2012) 647–652.
[19] J. Li, Y. Zhao, H.S. Tan, Y. Guo, C.-A. Di, G. Yu, Y. Liu, M. Lin, S.H. Lim, Y. Zhou, H. Su, B.S. Ong, Sci. Rep. 2 (2012).
[20] C.B. Nielsen, M. Turbiez, I. McCulloch, Adv. Mater. 25 (2013) 1859–1880.
[21] D. Chandran, K.-S. Lee, Macromol. Res. 21 (2013) 272–283.
[22] J.L. Brédas, J.P. Calbert, D.A. da Silva Filho, J. Cornil, Proc. Natl. Acad. Sci. U. S. A. 99 (2002) 5804–5809.
[23] T.D. Anthopoulos, G.C. Anyfantis, G.C. Papavassiliou, D.M. de Leeuw, Appl. Phys. Lett. 90 (2007).
[24] W.S. Yoon, S.K. Park, I. Cho, J.-A. Oh, J.H. Kim, S.Y. Park, Adv. Funct. Mater. 23 (2013) 3519–3524.
[25] B. Fu, J. Baltazar, A.R. Sankar, P.-H. Chu, S. Zhang, D.M. Collard, E. Reichmanis, Adv. Funct. Mater. (2014), http://dx.doi.org/10.1002/adfm.201304231.
[26] B. Sun, W. Hong, Z. Yan, H. Aziz, Y. Li, Adv. Mater. (2014), http://dx.doi.org/10.1002/adma.201305981.
[27] D.A. Egger, F. Rissner, E. Zojer, G. Heimel, Adv. Mater. 24 (2012) 4403–4407.
[28] C.-L. Wang, J. Wang, F.-Q. Bai, J. Chen, H.-X. Zhang, Int. J. Quantum Chem. (2014), http://dx.doi.org/10.1002/qua.24611.
[29] J.C. Bijleveld, A.P. Zoombelt, S.G.J. Mathijssen, M.M. Wienk, M. Turbiez, D.M. de Leeuw, R.A.J. Janssen, J. Am. Chem. Soc. 131 (2009) 16616–16617.
[30] P. Sonar, S.P. Singh, Y. Li, M.S. Soh, A. Dodabalapur, Adv. Mater. 22 (2010) 5409–5413.
[31] L. Dou, J. Gao, E. Richard, J. You, C.-C. Chen, K.C. Cha, Y. He, G. Li, Y. Yang, J. Am. Chem. Soc. 134 (2012) 10071–10079.
[32] X. Wang, S. Chen, Y. Sun, M. Zhang, Y. Li, X. Li, H. Wang, Polym. Chem. 2 (2011) 2872–2877.
[33] J. Liu, B. Walker, A. Tamayo, Y. Zhang, T.-Q. Nguyen, Adv. Funct. Mater. 23 (2013) 47–56.
[34] L. Fu, W. Fu, P. Cheng, Z. Xie, C. Fan, M. Shi, J. Ling, J. Hou, X. Zhan, H. Chen, J. Mater. Chem. A 2 (2014) 6589–6597.
[35] Z. Cai, Y. Guo, S. Yang, Q. Peng, H. Luo, Z. Liu, G. Zhang, Y. Liu, D. Zhang, Chem. Mater. 25 (2013) 471–478.
[36] J.C. Bijleveld, B.P. Karsten, S.G.J. Mathijssen, M.M. Wienk, D.M. de Leeuw, R.A.J. Janssen, J. Mater. Chem. 21 (2011) 1600–1606.
[37] G.E. Park, J. Shin, D.H. Lee, T.W. Lee, H. Shim, M.J. Cho, S. Pyo, D.H. Choi, Macromolecules 47 (2014) 3747–3754.
[38] A.D. Miller, S.A. Johnson, K.A. Tupper, J.L. McBee, T.D. Tilley, Organometallics 28 (2009) 1252–1262.
[39] D. Gendron, P.-O. Morin, P. Berrouard, N. Allard, B.R. Aïch, C.N. Garon, Y. Tao, M. Leclerc, Macromolecules 44 (2011) 7188–7193.
[40] B.L. Lucht, M.A. Buretea, T.D. Tilley, Organometallics 19 (2000) 3469–3475.
[41] G.L. Gibson, T.M. McCormick, D.S. Seferos, J. Am. Chem. Soc. 134 (2011) 539–547.
[42] G.L. Gibson, T.M. McCormick, D.S. Seferos, J. Phys. Chem. C 117 (2013) 16606–16615.
[43] Z. Cai, H. Luo, X. Chen, G. Zhang, Z. Liu, D. Zhang, Chem. Asian J. 9 (2014) 2.
[44] V.S. Gevaerts, E.M. Herzig, M. Kirkus, K.H. Hendriks, M.M. Wienk, J. Perlich, P. Müller-Buschbaum, R.A.J. Janssen, Chem. Mater. 26 (2013) 916–926.
[45] J. Liu, Y. Zhang, H. Phan, A. Sharenko, P. Moonsin, B. Walker, V. Promarak, T.-Q. Nguyen, Adv. Mater. 25 (2013) 3645–3650.
[46] W. Li, K.H. Hendriks, W.S.C. Roelofs, Y. Kim, M.M. Wienk, R.A.J. Janssen, Adv. Mater. 25 (2013) 3182–3186.
[47] W. Li, K.H. Hendriks, A. Furlan, W.S.C. Roelofs, M.M. Wienk, R.A.J. Janssen, J. Am. Chem. Soc. 135 (2013) 18942–18948.
[48] I. Meager, R.S. Ashraf, S. Rossbauer, H. Bronstein, J.E. Donaghey, J. Marshall, B.C. Schroeder, M. Heeney, T.D. Anthopoulos, I. McCulloch, Macromolecules 46 (2013) 5961–5967.
[49] C. Mitsui, J. Soeda, K. Miwa, H. Tsuji, J. Takeya, E. Nakamura, J. Am. Chem. Soc. 134 (2012) 5448–5451.
[50] H. Ebata, E. Miyazaki, T. Yamamoto, K. Takimiya, Org. Lett. 9 (2007) 4499–4502.
[51] Y. Kim, S. Cook, J. Kirkpatrick, J. Nelson, J.R. Durrant, D.D.C. Bradley, M. Giles, M. Heeney, R. Hamilton, I. McCulloch, J. Phys. Chem. C 111 (2007) 8137–8141.
[52] J.S. Kim, Y. Lee, J.H. Lee, J.H. Park, J.K. Kim, K. Cho, Adv. Mater. 22 (2010) 1355–1360.
[53] J.K. Park, J. Jo, J.H. Seo, J.S. Moon, Y.D. Park, K. Lee, A.J. Heeger, G.C. Bazan, Adv. Mater. 23 (2011) 2430–2435.
[54] C.H. Woo, P.M. Beaujuge, T.W. Holcombe, O.P. Lee, J.M.J. Fréchet, J. Am. Chem. Soc. 132 (2010) 15547–15549.
[55] A.T. Yiu, P.M. Beaujuge, O.P. Lee, C.H. Woo, M.F. Toney, J.M.J. Fréchet, J. Am. Chem. Soc. 134 (2011) 2180–2185.
[56] M. Wong, J. Hollinger, L.M. Kozycz, T.M. McCormick, Y. Lu, D.C. Burns, D.S. Seferos, ACS Macro Lett. 1 (2012) 1266–1269.
[57] J.R. Matthews, W. Niu, A. Tandia, A.L. Wallace, J. Hu, W.-Y. Lee, G. Giri, S.C.B. Mannsfeld, Y. Xie, S. Cai, H.H. Fong, Z. Bao, M. He, Chem. Mater. 25 (2013) 782–789.
[58] K.E. Horner, P.B. Karadakov, J. Org. Chem. 78 (2013) 8037–8043.
[59] T.M. Krygowski, H. Szatylowicz, O.A. Stasyuk, J. Dominikowska, M. Palusiak, Chem. Rev. (2014), http://dx.doi.org/10.1021/cr400252h.
[60] Y. Li, S.P. Singh, P. Sonar, Adv. Mater. 22 (2010) 4862–4866.
[61] J.C. Bijleveld, R.A.M. Verstrijden, M.M. Wienk, R.A.J. Janssen, J. Mater. Chem. 21 (2011) 9224–9231.
[62] J.W. Jung, J.W. Jo, F. Liu, T.P. Russell, W.H. Jo, Chem. Commun. 48 (2012) 6933–6935.
[63] Q. Peng, Q. Huang, X. Hou, P. Chang, J. Xu, S. Deng, Chem. Commun. 48 (2012) 11452–11454.
[64] Y. Li, P. Sonar, S.P. Singh, Z.E. Ooi, E.S.H. Lek, M.Q.Y. Loh, Phys. Chem. Chem. Phys. 14 (2012) 7162–7169.
[65] C.M. Cardona, W. Li, A.E. Kaifer, D. Stockdale, G.C. Bazan, Adv. Mater. 23 (2011) 2367–2371.
[66] Y. Wang, F. Yang, Y. Liu, R. Peng, S. Chen, Z. Ge, Macromolecules 46 (2013) 1368–1375.
[67] Y. Li, P. Sonar, S.P. Singh, M.S. Soh, M. van Meurs, J. Tan, J. Am. Chem. Soc. 133 (2011) 2198–2204.
[68] Y. Wen, Y. Liu, Y. Guo, G. Yu, W. Hu, Chem. Rev. 111 (2011) 3358–3406.
[69] S. Park, B.T. Lim, B. Kim, H.J. Son, D.S. Chung, Sci. Rep. 4 (2014).
[70] P. Sonar, S.P. Singh, E.L. Williams, Y. Li, M.S. Soh, A. Dodabalapur, J. Mater. Chem. 22 (2012) 4425–4435.
[71] M.S. Chen, O.P. Lee, J.R. Niskala, A.T. Yiu, C.J. Tassone, K. Schmidt, P.M. Beaujuge, S.S. Onishi, M.F. Toney, A. Zettl, J.M.J. Fréchet, J. Am. Chem. Soc. 135 (2013) 19229–19236.
[72] T. Schuettfort, L. Thomsen, C.R. McNeill, J. Am. Chem. Soc. 135 (2012) 1092–1101.
[73] J. Mei, D.H. Kim, A.L. Ayzner, M.F. Toney, Z. Bao, J. Am. Chem. Soc. 133 (2011) 20130–20133.
[74] H. Sirringhaus, P.J. Brown, R.H. Friend, M.M. Nielsen, K. Bechgaard, B.M.W. Langeveld-Voss, A.J.H. Spiering, R.A.J. Janssen, E.W. Meijer, P. Herwig, D.M. de Leeuw, Nature 401 (1999) 685–688.
[75] X. Guo, S.R. Puniredd, M. Baumgarten, W. Pisula, K. Müllen, J. Am. Chem. Soc. 134 (2012) 8404–8407.
[76] X. Guo, S.R. Puniredd, M. Baumgarten, W. Pisula, K. Müllen, Adv. Mater. 25 (2013) 5467–5472.
[77] P. Sonar, J.-M. Zhuo, L.-H. Zhao, K.-M. Lim, J. Chen, A.J. Rondinone, S.P. Singh, L.-L. Chua, P.K.H. Ho, A. Dodabalapur, J. Mater. Chem. 22 (2012) 17284–17292.